Thermal runaway behaviour of VRLA batteries

Robert K. Jaworski* and John M. Hawkins

Telstra Research Laboratories
770 Blackburn Rd., Clayton, Vic 3168, Australia

*Bell Communications Research
331 Newman Springs Rd., Red Bank, NJ 07701, USA

Abstract

This paper presents results from experiments of high resolution mapping of the internal temperatures of VRLA batteries on float duty. The internal thermal conditions of monoblock AGM VRLA batteries during different operating conditions have been characterised. The dynamic behaviour of the batteries during thermal runaway is reported. Changes of internal and external conditions leading to thermal runaway are discussed in terms of perturbation of the steady state conditions of the series-connected cells.

Introduction

The attributes of higher density and equipment compatibility have the valve-regulated lead-acid (VRLA) battery emerging as the technology of choice for standby applications in telecommunications. There is now a general trend away from the concentration of power plant in the controlled environments of the central office towards a much greater geographical decentralisation of power and back-up batteries. However, decentralised power plant is often installed in less controlled operating environments and the thermal behaviour of VRLA batteries used for backup power purposes under varied ambient conditions is of concern. Telstra operates battery-backed power plant in varied climatic conditions throughout Australia. It is therefore important to understand the service-life implications of VRLA batteries in uncontrolled environments and the subsequent risks to the Telstra network.

The thermal behaviour of VRLA batteries has received considerable attention in the context of both service-life and thermal runaway [1-9]. Thermal runaway of VRLA batteries describes the condition where the rate of heat generation within the battery exceeds its heat dissipation capacity, and is often linked to charging abuse or high ambient operating temperatures. For batteries on float service, thermal runaway is characterised by a co-operative increase in both charging (float) current and internal battery temperature over time which may lead to catastrophic and destructive failure. Evolution of hydrogen sulfide has also been reported during thermal runaway events [11]. System conditions believed to be conducive to thermal runaway have been described and many thermal management strategies have been advocated [6,9,12]. The physical geometry and internal design of the VRLA battery and the design of the battery installations contribute to the susceptibility of thermal runaway [3,4,10]. Current-limited float charging or temperature compensation of the float voltage are often proposed as important in alleviating the risk of thermal runaway [5,10,12]. However, either technique may not be easily applied in existing standby installations.

Thermal runaway may be difficult to predict and the causative agents often difficult to determine. It is therefore of interest to understand the conditions within an VRLA cell or battery which might exist prior to an thermal runaway episode. However, information about the thermal conditions and temperature distributions inside monoblock designs during both normal and abnormal operating conditions is limited [4,8,13]. This Paper describes some of the results to date of a program of study to better understand the thermal behaviour of production monoblocks used in Telstra's network subjected to varied operating conditions. High resolution measurement of the internal temperature gradients and float parameters has been used to characterise battery system conditions prior to thermal runaway. Monoblock batteries have been used to provide a simple model for the performance of series connected cells. It has been found that the susceptibility of the batteries to initiate and sustain thermal runaway episode is determined by several factors. Factors which affect the internal heat generation of a cell or monoblock within a battery string can be considered in terms of "perturbations" to the apparent thermal stability.

Perturbations of the normal operating conditions results in an interplay of the contributions of the series-connected cells which will determine whether thermal runaway will develop.

Experimental.

Thermal mapping and thermal runaway experiments were carried out in the laboratory on production 6V 100 Ah monoblock AGM VRLA batteries of the type used in the Telstra network. The monoblocks where all cubic in geometry, with an edge length of approximately 20 cm. While the comparative thermal behaviour and performance of similar VRLA batteries from different manufacturers is outside the scope of this paper, the results reported herein have been observed for all three different makes of VRLA batteries and thus the behaviour described may be considered generic.

Thermocouples, precision-placed to define the spatial volume of the monoblock VRLA battery, were used to accurately map thermal gradients within the battery during various operating conditions in environmental chambers. The internal temperature profiles were determined from internal plate temperatures measured at 28 different locations of each battery by calibrated temperatures probes inserted and sealed in precision-placed drill holes in the battery case. The probes were constructed using T-type thermocouples sealed in thin-wall glass tubing. Temperature measurements were accurate to 0.06°C or better over the temperature range of 15°C and 100°C. The temperature probes were positioned on the four sides of the monoblock parallel to the battery plates.

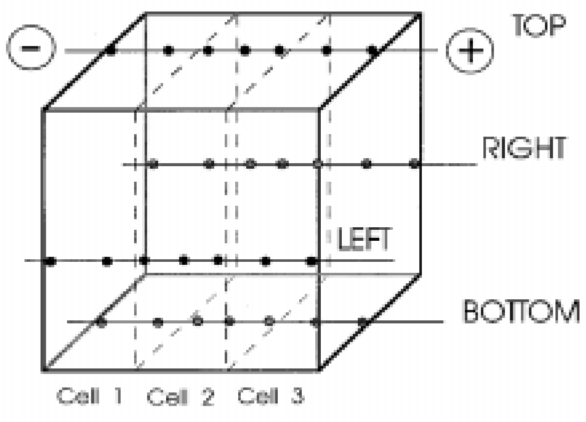

Figure 1: Location of 28 precision thermocouples in each 6V monoblock battery.

The probes were located so as to touch the edges of the plates and measure the temperature at four different locations of the same plate. *Figure 1* shows the positions of the thermocouples in each monoblock. Thermocouples were also positioned outside the monoblocks to monitor the ambient temperature.

All experiments were performed on fully charged batteries on constant voltage float placed in an environmental chamber which allowed ambient temperature control to better than 0.2°C. High resolution, computer controlled monitoring of the float current, float voltages, and thermocouples was used to track the float behaviour of the component cells within the monoblock as the batteries were subjected to different ambient temperature and float voltage conditions. A HP 6070A Power Supply was used for constant voltage float control. Battery current was determined from the voltage drop across a precision current shunt. Cell and monoblock potentials were directly measured. All data was collected under computer-control using a HP 3497A Data acqusition system using standard digital averaging techniques. Thermal runaway episodes were terminated by disconnection of the float charge circuit whenever the internal temperature of the monoblock exceeded 100°C. Single frequency impedance measurements of each of the cells in each monoblock were measured on a multiplexed and computer-controlled version of the Elcorp IMI801 single frequency battery impedance meter. Battery impedance behaviour during thermal runaway episodes is not reported in this paper.

Results and Discussion

Temperature Profiles

Thermocouple measurements of the operating temperatures of the plate edges provide a means to construct temperature profile “slices” of the inside of the monoblocks under various float conditions. Typical results are presented in series shown in *Figure 2* where the difference between the plate and external ambient temperatures *(ΔT)* is plotted as a function of spatial location within the monoblock *(floated at a constant 2.25V/cell)* for different external temperatures over the range of 25ºC to 65ºC.

As can be seen in *Figure 2*, the spatial temperature distribution within the monoblock is roughly parabolic and symmetric about the middle cell (cell 2). The middle cell always appears to operate at a higher temperature than either of the end cells. For lower ambient temperatures the sides of the measured plates appear to be isothermal. For higher operating temperatures, plate isothermal conditions are not maintained and, in generally, the top of the plates in each component cell is hotter than any other part of the plate. At 25ºC and 6.75V (2.25 V/cell), the internal plate temperature is only 0.2-0.3ºC higher than the surrounding external temperature. Even at the high ambient temperature of 65ºC, the highest inside temperature of the monoblock floating at 2.25V/cell is only about 3ºC higher than the external surroundings.

Figure 3 shows the temperature profiles for the same monoblock floated at 7.65V (2.55V/cell) at two different ambient temperatures (35°C and 45°C). The same basic parabolic shape of the temperature distributions across the battery is evident, but clearly the temperature differences between the inside and outside of the battery are much greater than for 2.25V/cell float conditions.

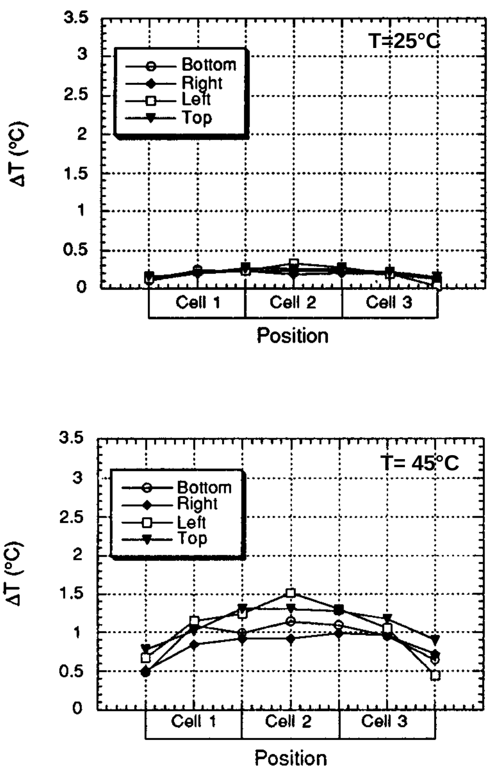

Figure 2: Temperature profiles for spatial slices of the monoblock at 6.75V (2.25V/cell) float control

Figure 2 and *Figure 3* indicate that under steady-state conditions over the temperatures and voltages ranges used, an increase in the control (float) voltage tends to result in larger difference between the internal and external battery temperature than does an increase in external operating temperature. This behaviour varies to some degree, depending on the physical construction of the monoblock. In practical terms, monoblocks such as these when subjected to significantly excessive float voltage can be expected to experience higher internal temperatures than the same monoblocks, correctly floated, exposed to the higher ambient temperatures which might be typically encountered in some of Telstra applications.

These results can be explained by a simplified thermal model of a monoblock where the relative temperature differences arise primarily from heat transfer characteristics across the plate-to-case interface. The heat transport properties of the plate edges are determined by the construction of the monoblock but are differentiated by the larger gas space above the plates. While details of the modelling are outside the scope of this paper, it is sufficient to conclude that it is possible to study thermal runaway events by analysing the temperature behaviour at a selected location in the battery. In this work, thermal runaway characteristics were studied by following the temperature profile of the location inside the monoblock exhibiting the highest temperature gradient.

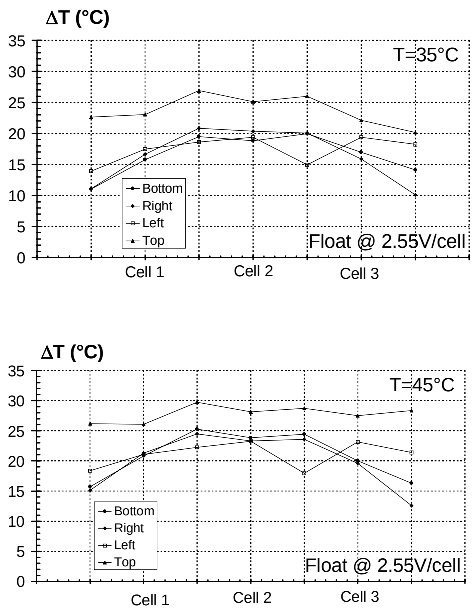

Figure 3: Typical temperature profiles for spatial slices of the monoblock at 7.65V (2.55V/cell) float control.

Thermal Runaway

Monoblocks could be forced into thermal runaway by a combination of time, elevated float voltage and ambient temperature. *Figure 4* shows data recorded during thermal runaway observed at 65°C when the applied voltage across the monoblock was stepped from 6.75V (2.25V/cell) to 7.80V (2.60V/cell.). The temperature-time profile of the thermocouple exhibiting the highest temperature difference above ambient and the battery current during the event are presented in *Figure 4a*. The voltage behaviour of the three individual cells in the monoblock is shown in *Figure 4b*. As can be seen from *Figure 4a*, thermal runaway is evident, and after about 8.5 hours, the internal battery temperature had reached 100°C. Of interest is that upon the voltage step, the current jumped immediately from its steady value of about 1A to over 16A, decaying to about 12A in response to establishing new equilibrium conditions at the higher applied voltage. After about 1.5 hours, the current passed by the battery begins to increase again, and just after 6 hours, begins a relatively steep non-linear increase so that after 8.5 hours, the battery is passing more than 25A. The internal temperature initially rises rapidly, but after two hours, the temperature increase has become virtually linear. As shown in *Figure 4b*, the individual cells polarise to different extents in response to the step in control voltage. Steady state cell voltages are established after about 2 hours and appear to be unaffected by the subsequent increase in battery current.

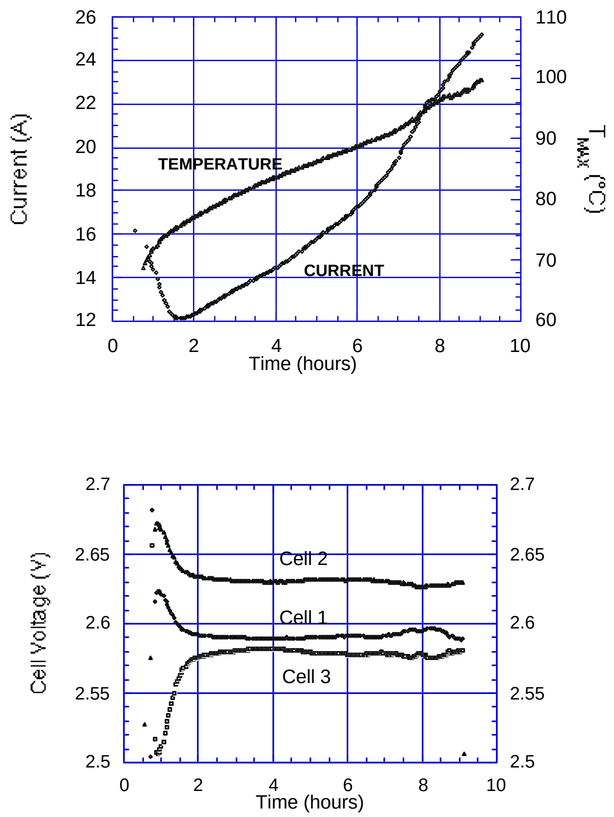

Figure 4: Typical thermal runaway behaviour at 2.6V/cell and 65ºC. (a) Battery current and temperature profile; (b) individual cell potential behaviour.

It is of note that Cell 2 (which is the hottest and which does enter runaway first) maintained the highest polarisation throughout the experiment.

The voltage step to 2.60V/cell represents a substantial voltage perturbation, and the 12A-16A passed by the battery represents a considerable Joule heating load. The onset of thermal runaway then was not particularly surprising. However, it was found that initiation of thermal runaway does not always require a large voltage change, and substantially slower current changes were observed to trigger a runaway condition. *Figure 4* illustrates the results from an experiment performed at an ambient operating temperature of 45ºC when the float control voltage was stepped from 6.75V (2.25V/cell) to 7.35V (2.45V/cell). As can be seen, the current taken by the battery decays from an initially high value resulting from the voltage step. As before, the temperature is seen to rapidly rise, presumably as a result of the IR heating originating from the increased current. As the current decays the rate of heat rise slows, but the heat generated in the battery now causes the current to increase. After 160 hours, the current had increased approximately linearly about two fold (from 2A to 4A), and the temperature of hottest part measured inside the monoblock had increased approximately linearly by only 9ºC. This corresponds to linear rates of current and internal temperature increases of about 14 mA/hour and about 0.06ºC/hour respectively.

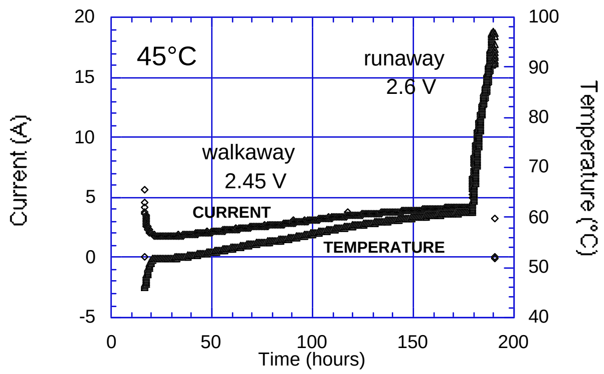

Figure 5: Typical example of thermal "walkaway". (a) battery current and temperature profile; (b) individual cell potentials.

These are very small changes which may easily go undetected in practical situations, particularly if measured over short time frames. However, these thermal "walkaways" may be common, and important transitional states. When the internal temperature has increased sufficiently, classical thermal runaway can be expected. Rapid thermal runaway can be precipitated by an additional voltage perturbation to the thermal walkaway condition. This is demonstrated in *Figure 5*, where, after about 180 hours, the control voltage was stepped to 7.80V (2.6V/cell). Thermal runaway was evident and the internal battery temperature reached 100ºC within 10 hours. The monoblock had previously failed to enter thermal runaway at 45ºC and 2.6V/cell, suggesting that the heat-load under the walkaway condition was a necessary precursor to trigger thermal runaway at this lower ambient temperature.

The importance of the pre-existing state as a determinant of thermal runaway conditions can be further considered with the results presented in *Figure 6* which shows the behaviour of the monoblock at 45ºC during the first 50 hours after a voltage step from 6.75V (2.25V/cell to 7.35V (2.45V/cell). *Figure 6a* illustrates the current and temperature response while *Figure 6b sho*ws the profile of the individual cell potentials over the same period.

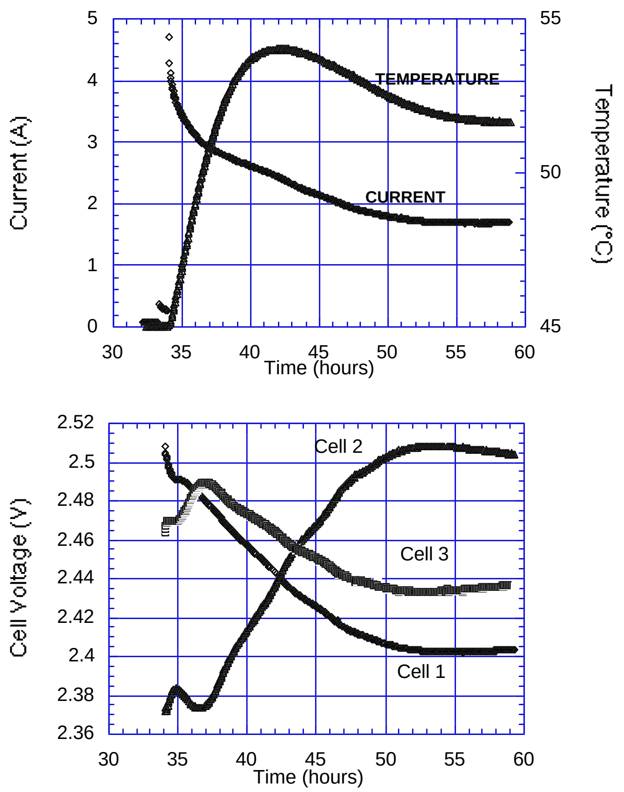

Figure 6: Typical example during first 60 hours of a thermal "walkaway"; (a) battery current and temperature profile; (b) individual cell potentials.

Of particular interest is that the temperature exhibits overshoot behaviour. Clearly, even though the current exponentially decays to a seemingly constant value after an initial rise in response to the voltage step, the battery undergoes significant heating throughout the apparent current stabilisation period. Yet thermal equilibrium is never attained, because, as indicated in *Figure 5*, the 200 mV/cell float voltage increase ultimately results in a slow, yet continuous temperature and current increase (*i.e.* thermal "walkaway"). The behaviour of the individual cells potentials also is of interest. As was the case in *Figure 4*, two of the three cells quickly polarise well above the nominal 2.45V/cell then decay over time as the current delays. The third cell however, cell 2 in this case, rises logarithmically. Unlike the situation in *Figure 5*, in this case there is no clear dominant cell behaviour, and some competing behaviour, or instability, is observed over the first five or so hours after the voltage step. Cell 2 finally emerges as the cell with the highest float potential and both the other two cells float below the nominal 2.45V/cell to compensate. The polarisation behaviour of the cells suggests that Cell 2 is not subject to IR heating initially to the same extent as the other two cells during the step of voltage, yet clearly Cell 2 does heat up and the monoblock does enter thermal walkaway. These results suggest that the degree of heating is not directly predictable. A cell with different float polarisation behaviour may or may not have entered thermal walkaway conditions more or less quickly.

It is clear that thermal runaway conditions do not have to immediately follow the perturbation, and apparent thermal instability may take some time to be manifest. Thermal runaway management strategies based solely on the magnitude of current flowing through the battery may not be very reliable. It appears that the rate of current increase and the rate of temperature increase are better indicators, but again incorrect conclusions may eventuate, depending on the time over which the rate of change are determined.

Thermal Maps

The temperature profiles provide spatial "slices" which can be used be used to construct 3-dimensional *thermal maps. Figure 7* shows two types of 3-D profiles of a the temperature of a representative point inside the monoblock as a function of ambient operating temperatures and float voltages. These maps provide an indication of the relative "ease" under which an battery in a particular steady state might be expected to enter thermal runaway. The "steepness" of the profile can be considered to represent a degree of robustness the monoblock displays against thermal runaway. These 3-D profiles allow comparison of the thermal performance of the different types monoblocks where battery design and construction can be expected to influence the thermal characteristics of the VRLA cell.

In this work, thermal runaway of monoblocks on float duty has been initiated by a significant perturbation to the external control (float) voltage. A voltage jump from 6.75V (2.25/Vcell) to 7.80V (2.6V/cell) represents the unlikely short-circuit failure of three 2V cells in a typical 48V telecommunications standby application.

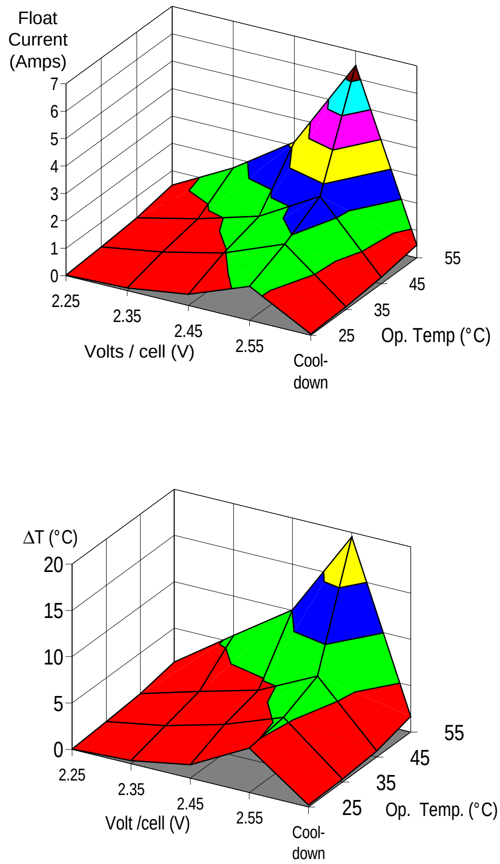

Figure 7 Example of 3-D Thermal maps for typical monoblocks showing (a) "float" current, and (b) maximum internal-external temperature difference, as a function of operating temperature and applied (float) voltages

Therefore, "fast" thermal runaway from the near simultaneous short-circuit cell failure is considered very unlikely for new VRLA of the type used in the Telstra network. In Telstra, rectifiers have a fail-safe operating range of 3% about the setpoint float voltage, so thermal runaway caused by large voltage perturbation arising from failed float control is also considered unlikely. However, the onset of thermal runaway from thermal walkaway of aged batteries is less fanciful. A voltage perturbation from 2.25V/cell to 2.45V/cell requires only two cells to fail. In-service situations, aged cell might be expected to fail sequentially in time, each thus applying increasing thermal load on thermal walkaway conditions. Changes in the external operating temperature may also be considered a source of perturbation of apparent steady-state conditions. Higher operating temperatures may not be sufficient to directly initial a ("fast") thermal runaway, but clearly may easily be adequate in contributing to the base internal heat load and thus place a the cell or monoblock in a state which is more susceptible to thermal walkaway. A more subtle perturbation to the existing thermal state is in the operation to the safety vent. Venting represent an intermittent heat loss mechanism and decreases the thermal mass of the battery [14]. Irregular and different vent operation on individual cells in a battery string over time can also be expected to contribute to the susceptibility towards thermal instability.

The results presented in this work deal with production monoblocks under external isothermal conditions, and the internal temperature profiles exhibit primarily symmetric spatial distributions about the centre cell. In practise, however, monoblock batteries are usually arranged in battery installations in spatial arrangement in which all cells may not experience dissipative symmetry. Depending on packing arrangements, cells may be located close and adjacent to other cells so that not all physical sides of the battery experience the same thermal environment. It is reasonably easy to contemplate packing and racking arrangements where the side or bottom (see *Figure 1*) have altered thermal interfaces so that the thermal characteristics of the cell or monoblock is no longer dominated by the under-lid gas space at the top of the battery. This may alter the thermal "symmetry" of the single monoblock and cause different thermal behaviour under perturbations which may lead to thermal runaway. The next stage of this work is to look at the effect of non-symmetrical thermal distributions on the *in-situ* thermal stability of VRLA in-service monoblocks.

Conclusion

High resolution internal temperature profiles of production monoblocks have been used to study and characterise conditions prior to a thermal runaway episode. It is proposed that for VRLA cells in series-connection string on standby duty, thermal runaway may be triggered by a perturbation of the steady state conditions. The perturbation may result in "typical" thermal runaway which is characterised by relatively rapid increase in battery current and internal battery temperature. Alternatively, much slower runaway conditions (thermal "walkaway") can also occur, where the increase in the battery float current or in the internal battery temperature is extremely slow. Walkaway conditions, which may precede a "normal" thermal runaway, are difficult to detect. Perturbation of the normal operating conditions results in an interplay of the contributions of the series-connected cells, which determines if thermal runaway will develop.

Internal temperature profiles and thermal maps have been used to help characterise differences in the thermal behaviour between different production monoblocks in the Telstra network. The mapping techniques are now being used to model the consequences of asymmetric heat dissipation behaviour of VRLA batteries packed in equipment housings operating in varied uncontrolled thermal environments in the network.

Acknowledgments

The authors would like to acknowledge the permission of the Director of Research, Telstra Research Laboratories, to publish this work.

References

1. R. Nelson, Intelec89, (1989), 12.6 pp. 1-8.
2. A. Takemasa, A. Kudou, S. Saito, A. Miura, T. , Hayakawa, and A. Komaki, *Progress in Batteries and Fuel Cells*, **8** (1989), pp. 217-220.
3. D. Berndt and E. Meissner, *Proc. Conf.* INTELEC 90, (1990), pp. 148-154.
4. R. Nelson, Intelec90, (1990), pp. 165-171.
5. Y.Nagai, K. Ozaki, Intelec90, pp. 155-160
6. S.D. Gerner, G.H. Brilmyer, and D.H. Bornemann, Intelec90, pp161-164
7. F. J. Vaccaro and R. E. Landwehrle, Intelec 91, (1991), pp. 20-25.
8. D. Calasanzio and D. McClelland, Intelec 92, pp. 22-27
9. S. S. Misra, T. N. Noveske, and A. W. Williamson, Intelec92, (1992)
10. A. I. Harrison, Intelec92, (1992), pp. 28-34.
11. R.S.Robinson and J.M.Tarascon, *J. Power Sources*, **48** (1993), pp 277-280.
12. H.D. Thacker, Intelec92, pp. 47-50
13. R.Frank, and G.Giess, Intelec 95, pp. 353-359.
14. D. Berndt, *Maintenance-Free Batteries*, John Wiley & Sonns, 1994, p 47.